

Article

How Sn(IV) Influences on the Reaction Mechanism of 11, *tri*-Butyl *p*-Coumarate and Its *tri*-Butyl-tin *p*-Coumarate Considering the Solvent Effect: A DFT Level Study

Rogelio A. Delgado-Alfaro * and Zeferino Gómez-Sandoval 

Facultad de Ciencias Químicas, Universidad de Colima, Km-9 Carretera Colima-Coquimatlán, Colima 28400, Mexico; zgomez@ucol.mx

* Correspondence: rogelio_delgado@ucol.mx

Abstract: Antioxidants are molecules that neutralize free radicals. In general, the reaction mechanisms of antioxidants are well known. The main reaction mechanisms of antioxidants are electron transfer (ET), hydrogen transfer (HT), and radical adduction formation (RAF). The study of these mechanisms is helpful in understanding how antioxidants control high free radical levels in the cell. There are many studies focused on determining the main mechanism of an antioxidant to neutralize a wide spectrum of radicals, mainly reactive oxygen species (ROS)-type radicals. Most of these antioxidants are polyphenol-type compounds. Some esters, amides, and metal antioxidants have shown antioxidant activity, but there are few experimental and theoretical studies about the antioxidant reaction mechanism of these compounds. In this work, we show the reaction mechanism proposed for two esters, 11, *tri*-butyl *p*-coumarate and its *tri*-butyl-tin *p*-coumarate counterpart, using Sn(IV). We show how Sn(IV) increases the electron transfer in polar media and the H transfer in non-polar media. Even though the nature of esters could be polar or non-polar compounds, the antioxidant activity is good for the Sn(IV)-*p*-coumarate complex in non-polar media.



Citation: Delgado-Alfaro, R.A.; Gómez-Sandoval, Z. How Sn(IV) Influences on the Reaction Mechanism of 11, *tri*-Butyl *p*-Coumarate and Its *tri*-Butyl-tin *p*-Coumarate Considering the Solvent Effect: A DFT Level Study. *Computation* **2023**, *11*, 220. <https://doi.org/10.3390/computation11110220>

Academic Editor: Aleksey E. Kuznetsov

Received: 27 July 2023

Revised: 13 September 2023

Accepted: 20 September 2023

Published: 3 November 2023



Copyright: © 2023 by the authors. Licensee MDPI, Basel, Switzerland. This article is an open access article distributed under the terms and conditions of the Creative Commons Attribution (CC BY) license (<https://creativecommons.org/licenses/by/4.0/>).

Keywords: reaction mechanism; solvent; antioxidant; metal influence; density functional theory

1. Introduction

Within the development of new compounds for the treatment of diseases or conditions influenced by oxidative stress, synthetic antioxidants such as 2(3)-11, *tri*-butyl-4-hydroxyanizole (BHA), 2,5-di-11, *tri*-butyl-4-hydroxytoluene (BHT) [1,2], and Edaravone [3], among others, have been developed and have been shown to have a good capacity as neutralizers of free radicals produced by oxidative stress. In addition to these compounds, a wide variety of compounds linked to metals like Sn(IV) have been developed, showing greater biological activity as antioxidants [4,5]. For the synthesized series, in vitro tests of the antioxidant activity against different substrates like 2,2-difenil-1-picrilhidrazil (DPPH), 2,2'-azino-bis(3-ethylbenzothiazoline-6-sulfonic acid radical cation (ABTS⁺), and ethylene diamine tetra-acetic acid (EDTA) have been carried out with different methodologies, but none of them simulating the cellular environment. Therefore, the results have shown that the antioxidant activity varies according to the selected method. There are few studies on the mechanism by which radical neutralization is carried out for this type of compound at an experimental and theoretical level [3].

To know the mechanism by which the neutralization of free radicals is carried out and its effectiveness, the chemical kinetics as described by the theory of the transition state [6–9] and the Marcus theory [10] are very useful. Among the reaction mechanisms studied in chemical kinetics are, electron transfer (ET), hydrogen transfer (HT), and radical adduct formation (RAF).

With the calculated values of the reaction energy ΔG^0 for each reaction channel (radical–molecule interaction site) and using the Marcus theory, the activation energy of

the electronic transfer mechanism ΔG^\ddagger is obtained. The value of the reaction rate constant k is calculated using the transition state theory for the mechanism of electron transfer and hydrogen abstraction. Since the ·OH and ·OOH radicals are transported in the cell medium by diffusion, an apparent rate constant k_{app} is thus preferred to model the electron transfer mechanism.

The objective of this work is to evaluate the antioxidant activity of 11, *tri*-butyl *p*-coumarate vs. *tri*-butyl-tin *p*-coumarate showing that the presence of the Sn(IV) in the *p*-coumarate contributes to improving the reaction mechanism and its efficiency as a radical neutralizer of ROS like ·OH and ·OOH, simulating the cellular environment.

Based on the results obtained for the calculation of ΔG^0 , it was found that reaction channel 4a (Figure 1) is the most favored for the radical–molecule interaction, showing that for the ET mechanism in a polar medium 11, *tri*-butyl-tin *p*-coumarate shows a k_{app} in the order of 10^7 and 10^8 vs. the ·OOH and ·OH radicals, respectively, with respect to the k_{app} values of 10^6 and 10^{-24} of 11, *tri*-butyl-*p*-coumarate against the ·OOH and ·OH radicals, respectively.

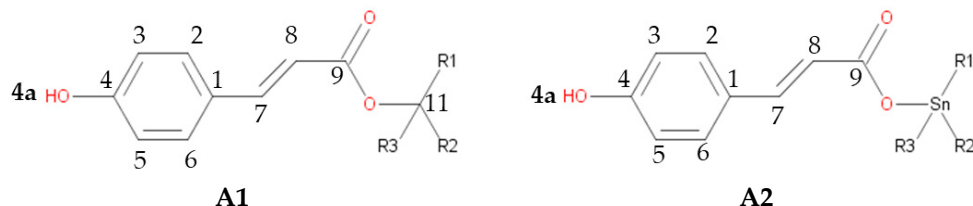


Figure 1. The 11, *tri*-butyl *p*-coumarate (**A1**) and *tri*-butyl-tin *p*-coumarate (**A2**) structures ($R_n = n$ -butyl, $n = 1, 2, 3$), where reaction channel **4a** is shown on the left for both molecules.

Regarding the HT mechanism, it was only possible to obtain data to calculate the k for the ·OOH radical, showing an order of 10^6 for both molecules in a polar medium, and of 10^3 and 10^5 in a nonpolar medium for 11, *tri*-butyl-*p*-coumarate and 11, *tri*-butyl-tin *p*-coumarate, respectively, showing that Sn(IV) contributes to increasing the reactivity in the 4a channel for the transfer of an H atom in the neutralization of ROS-type radicals such as ·OOH.

The evaluation of the antioxidant activity of both molecules is comparable with other previously studied antioxidants such as glutathione and propenesulfonic acid, whose k are in the order of 10^7 for both in a polar medium for the ET mechanism and 10^3 for the HT mechanism in a nonpolar and polar medium.

We concluded that the presence of Sn(IV) in the *p*-coumarate ester molecule seems to contribute to increasing the reactivity in reaction channel 4a, with the most efficient mechanisms being ET in polar media and HT in non-polar media.

2. Computational Details

The Khon–Sham approximation for Density Functional Theory [11,12], as implemented in Gaussian 09 [13], was the method of choice for the present study. The Truhlar M05 functional [14] was employed as well. The 6-311+G (d, p) [15] basis set for N, O, C, and H atoms, along with LANL2DZ pseudo-potentials and basis set [16–18] for Sn(IV) atom were also employed. The M05 functional has been recommended for kinetics calculation by its developers for systems that commonly present a multireference character, and it has been successfully used by independent authors for that purpose [19–23]. Full geometry optimization for *p*-coumaric esters (Figure 1) was performed without symmetry constraints. Harmonic frequency analysis was made to verify optimized local minima and transition states at the potential energy surface. Local minima have only real frequencies, while transition states have one imaginary frequency (I.F.) that corresponds to the expected motion along the reaction coordinate.

Relative energies are computed with respect to the sum of the separated reactants. Solvent effects are considered by employing the SDM continuum model [24] using wa-

ter and pentylethanoate as solvents, to mimic de cellular environment and describe the molecular and biological systems and their properties. The solvent cage effect has been considered according to the correction proposed by Okumo [25], taking into account the free energy volume theory [26]. Both corrections described above are in good agreement with those obtained by Ardura et al. [27] and successfully used by other authors [28–34]. The expression used to correct ΔG^0 is:

$$\Delta G_{sol}^{FV} \cong \Delta G^0 - RT \left\{ \ln \left[n \cdot 10^{(2n-2)} \right] - (n-1) \right\}, \quad (1)$$

where n is the molecularity of the reaction. According to Equation (1), the cage effect in solution causes ΔG^0 to decrease by 2.54 kcal/mol for bimolecular reactions, at 298.15 K.

The rate constant k was computed employing the conventional transition state theory (TST) [35–37] and the 1 M standard state as:

$$k = \sigma \tau \frac{k_B T}{h} e^{-(\Delta G^\ddagger)/RT}, \quad (2)$$

where k_B and h are the Boltzmann and Plank constants, respectively, T is the absolute temperature in K, R is the universal gas constant, ΔG^\ddagger is the activation energy, σ represents the reaction path degeneracy (accounting for the number of equivalent reaction paths), and τ accounts for the tunneling correction (defined as the Boltzmann average of the ratio of the quantum and the classical probabilities). ΔG^\ddagger and τ were computed using the zero-curvature tunneling correction (ZCT) [38]. TST has proven to be appropriate for describing chemical reactions between free radicals and antioxidants [39].

For the mechanism involving a single ET, the Marcus theory was employed [40,41] to calculate ΔG^\ddagger in terms of two thermodynamic parameters: ΔG^0 and the nuclear reorganization energy (λ)

$$\Delta G_{ET}^\ddagger = \frac{\lambda}{4} \left(1 + \frac{\Delta G_{ET}^0}{\lambda} \right)^2, \quad (3)$$

where λ is calculated as:

$$\lambda = \Delta E_{ET} - \Delta G_{ET}^0, \quad (4)$$

with ΔE_{ET} being the ou11, tri-sphere reorganization energy (that reflects changes in the polarization of solvent molecules during electron transfer) computed as the vertical non-adiabatic energy difference between reactants and products. Some of the calculated rate constant values are close to the diffusion limit. Accordingly, TST calculations cannot directly obtain the apparent rate constant. In the present work, the Collins–Kimball Theory [42] is used to correct the rate constant, and k_{app} is calculated as:

$$k_{app} = \frac{k_D k_T}{k_D + k_T}, \quad (5)$$

where k_T is the thermal rate constant computed by the TST calculation, and k_D is the steady-state Smoluchowski rate constant [43] for an irreversible bimolecular diffusion-controlled reaction:

$$k_D = 4\pi R D_{AB} N_A, \quad (6)$$

where R denotes the reaction distance, N_A is the Avogadro number, and D_{AB} is the mutual diffusion coefficient of the reactants A (free radical) and B (**A1** and **A2**). D_{AB} is computed from D_A and D_B according to reference [44], being D_A and D_B estimated from the Stokes–Einstein approach [45]:

$$D = \frac{k_B T}{6\pi\eta a}, \quad (7)$$

where T is the temperature, η the viscosity of the solvent (in our case water, $\eta = 8.91 \times 10^{-4}$ Pa s, and pentylethanoate, $\eta = 8.62 \times 10^{-4}$ Pa s), and a is the radius of the solute.

Direct reaction branching ratios (Γ) are computed as:

$$\Gamma_{path} = \frac{k_{path}}{k_{overall}} \times 100. \quad (8)$$

We have chosen the average reported pK_a (the negative log of the acid dissociation constant value) for *p*-coumaric acid of 4.38 [46] as the reference $pK_{a_{ref}}$, to compute the theoretical pK_a for 11, *tri*-butyl *p*-coumarate and *tri*-butyl-tin *p*-coumarate by using the method proposed by Ho [47]

$$pK_a = \frac{\Delta G_{ani}^0}{RTLn(10)} + (pK_{a_{ref}}), \quad (9)$$

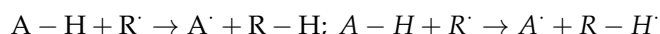
where ΔG_{ani}^0 is the free energy for the anion formation. Thus, in an aqueous solution at pH = 7.4, the neutral form of 11, *tri*-butyl *p*-coumarate (**A1**), and *tri*-butyl-tin *p*-coumarate (**A2**) would predominate (97.7% and 97.6% respectively) over the deprotonated forms (A_1^- 2.3% and A_2^- 2.4%, respectively). In this work, both neutral and deprotonated forms will be used to study their reactivity toward the considered free radicals in water, while in lipid media only the neutral form will be considered.

3. Results and Discussion

Reaction mechanism and kinetics for 11, *tri*-butyl *p*-coumarate ester and its counterpart *tri*-butyl tin-*p*-coumarate ester were computed for the structures shown in Figure 1. Once optimized ester geometries are obtained, the multireference character is determined by a single point calculation employing the CCSD method to compute the T1 parameter. The T1 parameter is used to determine the multireference character of an organometallic complex [48,49]. For neutral molecules, if the T1 value is higher than 0.023, they have a multireference character, and for transition state geometries if T1 is higher than 0.044, they have a multireference character. The T1 values for both **A1** and **A2** were 0.032.

The theoretical calculations performed in this work agree with the following reaction mechanisms:

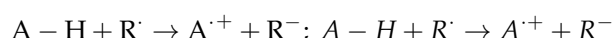
1. Hydrogen transfer (HT)



2. Radical adduct formation (RAF)



3. Single electron transfer from neutral form (SET-1)



4. Single electron transfer from deprotonated form (SET-2)



The SET-1 mechanism considers the neutralization of the free radical from the neutral structure, and in this mechanism, the electron transfer to the radical is carried out, with which the antioxidant remains as a radical cation and the radical as anion.

The SET-2 mechanism considers the neutralization of the radical from the anionic form of the antioxidant, and in this case, the antioxidant remains as a radical and the radical as an anion.

For both cases, the radical formed can enter a regeneration route to reform the neutral molecule or the anion, respectively. With respect to the radical, this can be neutralized by the free protons in the medium.

In the HT mechanism, we have considered the H atom abstraction from the hydroxyl group at position 4, and the abstraction of the H atoms bounded to C at positions 7 and 8.

The object of the present work was to determine how the presence of the Sn(IV) influences the different reaction mechanisms and their rate constants in the reaction of **A1** and **A2** with the ·OOH and ·OH free radicals, in water and lipid media. The thermochemical feasibility of the different reaction mechanisms and channels was investigated first since it determines the viability of the chemical process.

For **A1** and **A2** molecules, *pKa* values, mol fraction in aqueous solution, and bond dissociation energy (BDE) for hydrogen atoms on reaction channels 7 (C7), 8 (C8) and 4a (·OH on C4), in water and pentylethanoate media, were computed and the results are shown in Table 1.

Table 1. *pKa*, mol fraction in aqueous solution and bond dissociation energy (BDE) in kcal/mol for **A1** and **A2** molecules.

	A1_(I)	A1_(II)	A2_(I)	A2_(II)
<i>pKa</i>	9.011	-	9.014	-
Mol frac.	0.023	-	0.024	-
Channel	BDE			
4a	70.53	76.61	70.90	70.59
7	89.85	90.92	91.49	90.80
8	100.33	98.70	164.65	99.64

(I) = water, (II) = pentylethanoate.

BDE for channel 4a showed the lowest value compared to reaction channels 7 and 8; thus, channel 4a is energetically the most viable for **A1** and **A2**. BDE for molecule **A2** slightly increases with the presence of the Sn(IV) moiety.

3.1. Single Electron Transfer (SET) Mechanism

ΔG^0 for the **SET-1** and **SET-2** mechanisms, calculated at 298.15 K in solution with ·OOH and ·OH radicals, are shown in Table 2.

Table 2. Reaction energy ΔG^0 in kcal/mol, with the ·OOH and ·OH radicals, in water and pentylethanoate, at 298.15 K.

	A1_(I)		A1_(II)		A2_(I)		A2_(II)	
	·OOH	·OH	·OOH	·OH	·OOH	·OH	·OOH	·OH
SET-1	26.04	0.62	64.88	41.35	26.54	0.82	68.21	44.67
SET-2	2.62	−22.97	−	−	0.81	−24.91	−	−

(I) = water, (II) = pentylethanoate.

For the **SET-1** mechanism (Figure 2a), where the radical cation is formed from neutral geometry, ΔG^0 with the radical ·OOH in an aqueous solution is highly endergonic for both reactions with **A1** and **A2**, so these reactions are not viable. With ·OH radical, the reactions are slightly endergonic. ΔG^\ddagger values for **A2** reaction with ·OH radicals decrease compared to **A1**. The order of the apparent rate constant k_{app} for reactions of **A1** and **A2** with ·OH radical doesn't change, $10^9 \text{ M}^{-1} \text{ s}^{-1}$, showing that the presence of the Sn(IV) in **A2** contributes to decrease the height of the energy barrier but not to decrease the width, which is essential in the electron tunnel effect, but this contribution do not influence to improve the antioxidant activity.

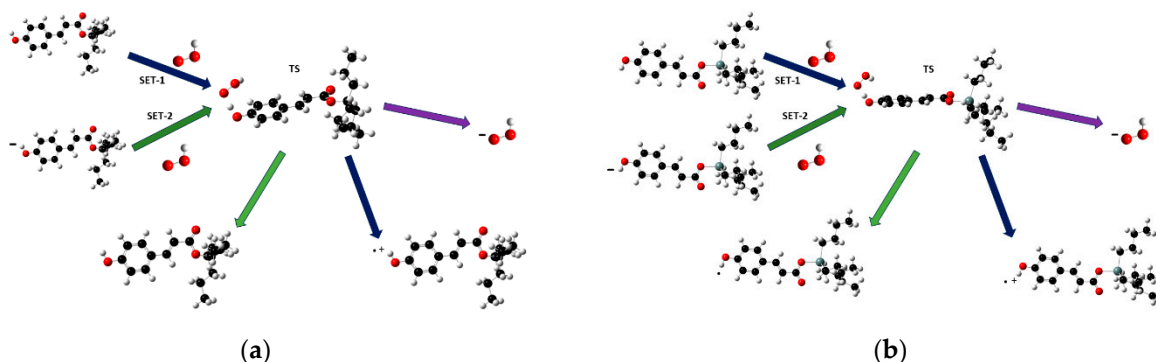


Figure 2. (a) SET-1 and SET-2 mechanism illustration for **A1**, (b) SET-1 and SET-2 mechanism illustration for **A2**.

In pentylethanoate, ΔG^0 is highly endergonic with both ·OOH and ·OH radicals because the formation of the ionic species is not viable. Since the SET-1 mechanism shows an endergonic ΔG^0 of **A1** and **A2** with the OOH and ·OH radical, these values are normal in the nonpolar medium (pentylethanoate) since the formation of the cation is not viable; on the contrary, in the polar medium (water), the formation of the cation by charge transfer would mean viability for its formation, but due to the ΔG^0 values shown, it is not. This may be due to the presence of the tert-butyl and tert-butyl-tin group acts as an electro-acceptor group in the molecule with neutral geometry, which can contribute to a decrease in the electron density in the aromatic ring, decreasing the ability of the charge to be transferred to the radical when interacting with the antioxidant.

For the SET-2 mechanism (Figure 2b), ΔG^0 is endergonic with the radical ·OOH and highly exergonic with the radical ·OH. For **A2**, which has a Sn(IV), ΔG^0 is less endergonic in the reaction with ·OOH radical and more exergonic with ·OH radical, compared to the **A1** reaction. It is shown that the organometallic moiety acts like an electron-donor group, donating electron density to the ester in its deprotonated form favoring the charge transfer, opposite to the development of the SET-1 mechanism.

ΔG^\ddagger values for the **A2** reaction with ·OOH radical slightly decrease compared to the **A1** reaction. On the other hand, in the reaction of **A2** with ·OH radical, ΔG^\ddagger decreases considerably compared to the **A1** case. The comparison is summarized in Table 3.

Table 3. Activation energy ΔG^\ddagger in kcal/mol, the apparent rate constant k_{app} in $M^{-1} s^{-1}$.

	A1_(I)		A2_(I)	
SET-1	ΔG^\ddagger	k_{app}	ΔG^\ddagger	k_{app}
·OOH	-	-	-	-
·OH	1.28	8.55×10^9	0.34	8.78×10^9
SET-2	ΔG^\ddagger	k_{app}	ΔG^\ddagger	k_{app}
·OOH	4.65	1.25×10^6	4.03	9.13×10^7
·OH	44.41	8.53×10^{-24}	28.40	2.12×10^8

(I) = water.

For k_{app} of **A1** and **A2** reactions, with ·OOH and ·OH radicals, the order increases from $10^6 M^{-1} s^{-1}$ to $10^7 M^{-1} s^{-1}$ for the reactions with ·OOH, and from $10^{-24} M^{-1} s^{-1}$ to $10^8 M^{-1} s^{-1}$ for the reactions with ·OH. Therefore, the presence of Sn(IV) contributes to improving the reactivity of the ester increasing its efficiency like an antioxidant. The order of k_{app} for **A2** with the radical ·OOH is comparable to the one shown by glutathione ($2.7 \times 10^7 M^{-1} s^{-1}$) [50] and the propensulphonic acid ($2.6 \times 10^7 M^{-1} s^{-1}$) [51].

3.2. Hydrogen Transfer (HT) Mechanism

ΔG^0 for the HT mechanism, regarding reaction channels 4a, 7, and 8 in aqueous media, are shown in Table 4. For the A1 and A2 reactions with radical ·OOH, ΔG^0 for reaction channels 7 and 8 is endergonic in both aqueous and lipid media. In reaction channel 7 ΔG^0 increases in water and decreases in lipid media with the presence of Sn(IV), which shows that the presence of Sn(IV) favored the reaction in lipid media. For reaction channel 8, the presence Sn(IV) on A2 contributes to increase ΔG^0 in both water and lipid media. Therefore, reaction channel 8 is the less favored.

Table 4. Reaction energy ΔG^0 in kcal/mol for A1 and A2 esters with radical ·OOH and ·OH.

	A1 _(I)	A1 _(II)	A2 _(I)	A2 _(II)
4a				
·OOH	−6.65	1.75	−6.27	−4.27
·OH	−41.92	−33.94	−42.04	−39.97
7				
·OOH	12.67	16.06	14.31	15.93
·OH	−23.09	−19.64	−21.46	−19.76
8				
·OOH	23.16	23.85	87.47	24.79
·OH	−12.11	−11.86	51.71	−10.92

(I) = water, (II) = pentylethanoate.

On the other hand, ΔG^0 in reaction channels 7 and 8 is exergonic for reactions with ·OH radical, except for A2 on water, where ΔG^0 is highly endergonic. In aqueous and lipid media, an increase in ΔG^0 for reaction channel 7 for A2 is shown in the presence of Sn(IV) compared to the A1 reaction. For reaction channel 8, ΔG^0 is exergonic for A1 in water and lipid media. For A2, the presence of the Sn(IV) increases considerably ΔG^0 in water media. In lipid media, the presence of Sn(IV) on A2 contributes to increase ΔG^0 , showing that channel 7 is more viable than channel 8 and that the presence of the Sn(IV) contributes to the increase in ΔG^0 of the HT mechanism.

For reaction channel 4a (Figure 3a,b), ΔG^0 is exergonic for the reactions with radical ·OOH for A1 (except in lipid media) and A2. In water, ΔG^0 slightly increases with the presence of Sn(IV). In pentylethanoate, ΔG^0 is endergonic for A1, and exergonic when Sn(IV) is present for A2, showing that the presence of Sn(IV) influences the transferring of light atoms like H.

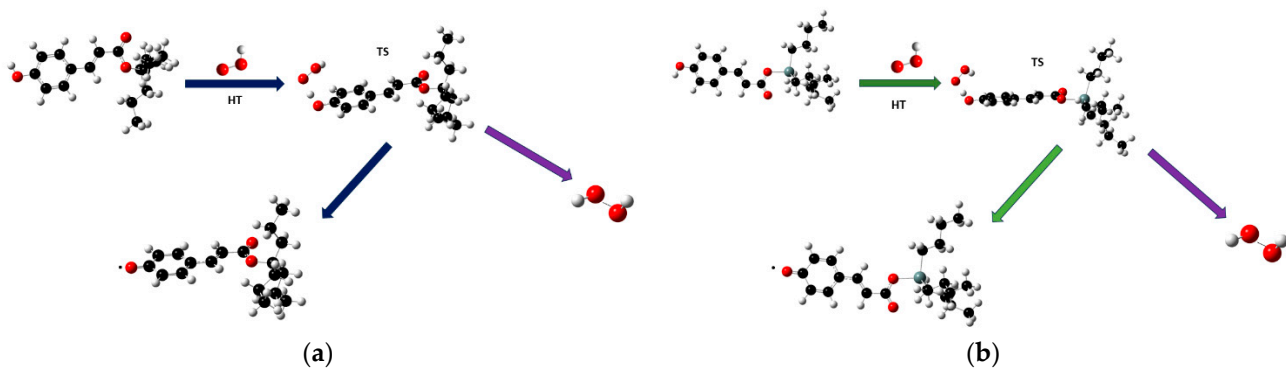


Figure 3. (a) HT mechanism illustration for A1, (b) HT mechanism illustration for A2.

For reaction with radical ·OH, ΔG^0 is exergonic, even higher than that shown on channels 7 and 8. Therefore, reaction channel 4a is the most viable in both pentylethanoate and water media. When Sn(IV) is included in the A2 reaction, ΔG^0 is more exergonic than for the A1 reaction, meaning that the presence of Sn(IV) contributes to increasing the hydrogen transfer in both media.

From the above, we can see that the 'OOH radical is highly selective with the functional groups with which it interacts, we can see that sites 7 and 8 are carbons with sp^2 hybridization which have an electron-donating character, but cannot release the electron to neutralize to the radical, so the 'OH group that does have the ability to donate an electron to the radical is the most viable.

For the HT mechanism, transition state geometries were optimized for **A1** and **A2** with the 'OOH radical, verifying that each transition state has an imaginary frequency corresponding to the reaction coordinate (Figure 4). Transition state geometries, for reaction with 'OH radical, cannot be obtained. Although their ΔG^0 values are highly exergonic, it is probable that the reaction is carried out by diffusion.

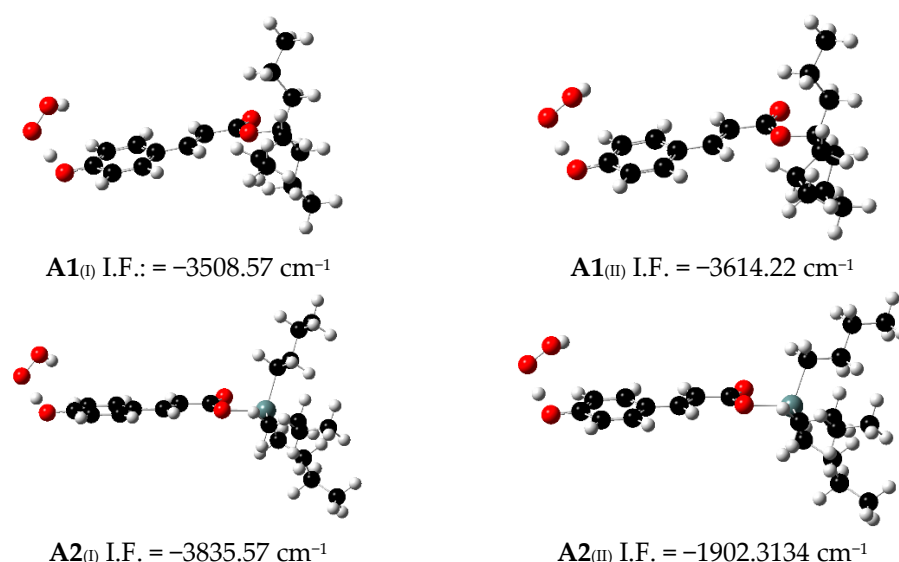


Figure 4. Optimized transition state geometry of **A1** and **A2** with radical 'OOH in water (I) and pentylethanoate (II) and their imaginary frequencies (I.F.).

Activation energy ΔG^\ddagger and rate constant k for **A1** and **A2** molecules in aqueous and lipid media were computed and are shown in Table 5. For **A1** and **A2** reactions with 'OOH radical on water, computed values of ΔG^\ddagger were 13.07 and 12.26 kcal/mol, respectively. For k computed values were 1.24×10^6 and $4.64 \times 10^6 \text{ M}^{-1} \text{ s}^{-1}$, for **A1** and **A2**, respectively. Although the presence of the Sn(IV) for **A2** contributed to a decrease in the ΔG^\ddagger barrier, the order of magnitude for k remains without change. It can be due to the presence of the metal, which contributes to decreasing the activation energy barrier, but does not contribute to modifying the width of the barrier during the tunnel effect through the HT.

Table 5. Activation energy barrier ΔG^\ddagger in kcal/mol and rate constant k in $\text{M}^{-1} \text{ s}^{-1}$ for **A1** and **A2** molecules in aqueous and lipid media.

	A1(I)		A1(II)		A2(I)		A2(II)	
	ΔG^\ddagger	k						
'OOH	13.07	1.24×10^6	18.47	4.12×10^3	12.26	4.64×10^6	12.56	1.25×10^5

(I) = water, (II) = pentylethanoate.

In pentylethanoate, ΔG^\ddagger values for **A1** and **A2** reactions were 18.47 and 12.56 kcal/mol, respectively, and computed k values were $4.12 \times 10^3 \text{ M}^{-1} \text{ s}^{-1}$ for **A1** and $1.25 \times 10^5 \text{ M}^{-1} \text{ s}^{-1}$ for **A2**. In the non-polar phase, it was shown that Sn(IV) contributes to decreasing the activation barrier improving the tunnel effect, and increasing the rate order on **A2**, meaning that the presence of the metal contributes to improving its efficiency like an antioxidant on this type of system.

This finding is extremely important since the Sn(IV) ester in its neutral form presents a greater facility to release a hydrogen atom when interacting with a radical, which can be beneficial when interacting with membrane proteins and participating in a repair process in an essential site of the protein structure or cause possible damage to the protein by modifying its function, this opens the way to study in depth the interaction with membrane proteins.

3.3. Reaction Adduct Formation (RAF)

In Table 6, the computed values of the total rate constant k_{Tot} are shown. The contribution of each rate constant for electron transfer and hydrogen transfer mechanism was included for 'OOH and 'OH radicals.

Table 6. Total rate constant k_{Tot} in $M^{-1} s^{-1}$ for **A1** and **A2** molecules in aqueous and lipid media.

	A1_(I)	A1_(II)	A2_(I)	A2_(II)
'OOH	2.5×10^6	4.12×10^3	9.59×10^7	1.25×10^5
'OH	8.55×10^9	-	8.99×10^9	-

(I) = water, (II) = pentylethanoate.

The contribution of each mechanism in the antioxidant activity of **A1** and **A2** was computed by calculating the contribution ratio:

$$\Gamma = \frac{k_i}{k_T} \times 100, \quad (10)$$

where Γ is the contribution ratio, k_i is the rate constant of the reaction mechanism and k_T is the total rate constant. Rate contributions to the antioxidant activity are represented as percentages in Table 7.

Table 7. Contribution (Γ) of each mechanism to the antioxidant activity.

	A1_(I)	A1_(II)	A2_(I)	A2_(II)
	Γ	Γ	Γ	Γ
SET-1				
'OOH	-	-	-	-
'OH	100		97.6	
SET-2				
'OOH	50	-	95.2	-
'OH	0	-	2.36	-
HT				
'OOH	49.6	100	4.84	100
'OH	-	-	-	-

(I) = water, (II) = pentylethanoate.

For the reaction of **A1** with 'OH radical, the main contribution comes from the SET-1 mechanism, which contributes 100%, due to the very low-rate order of k shown in the SET-2 mechanism. On the other hand, in the reaction with **A2**, the 'OH contribution is 97.6%. The lower contribution is due to the deprotonated species, which contributes 2.36%. This means that both esters are good antioxidants in their neutral form.

For the **A1** reaction with 'OOH radical, SET-2 and HT mechanisms contribute at almost the same rate, 50.4% and 49.6%, respectively. With respect to **A2**, the contribution changes due to the presence of Sn(IV), where the main contribution comes from the SET-2 mechanism with 95.2% and 4.84% from the HT mechanism, showing that the presence of Sn(IV) contributes to significantly increase the electron-donor character of the ester to neutralize peroxy radicals, but not the transfer of light atoms like H. In lipid media, the main contribution comes from the HT mechanism, since the ester cannot form ionic species.

This shows that metal could improve the antioxidant capability of the ester derived from *p*-coumaric acid against peroxy-type radicals.

The results obtained in this study are in line with those obtained experimentally, where metals such as Cu(II) [52], Ni(II), and Co(II) [53] contribute to improving the ability to neutralize free radicals of antioxidant compounds.

Although the findings of this work between compounds **A1** and **A2** show that the presence of Sn(IV) contributes to improving the antioxidant capacity, it is necessary to deepen the current study to determine more precisely the role played by Sn(IV) within the antioxidant structure; this is because the metal can be coordinated to the organic compound as a complex [54] or as a part of the compound [4], as is the current case.

4. Conclusions

The present study contributes to showing how the presence of Sn(IV) in an ester derived from the *p*-coumaric acid can contribute to increase or decrease its antioxidant capability. Due to the great electronegativity of the ·OH radical, **A2** reacts with the ester in its neutral form with and without the presence of the Sn(IV), as shown in the **SET-1** mechanism. In the presence of the metal, it is observed that the rate constant increases for the **SET-2** mechanism showing that Sn(IV) contributes to improving the antioxidant capability of the anion (deprotonated species), even though the main contribution comes from the **SET-1** mechanism. Similar behavior can be seen in the TH mechanism, where the presence of Sn(IV) does not contribute to improving the antioxidant capability. All the above in water. On the other hand, in lipid media the presence of the Sn(IV) has a great influence on the rate constant order, improving its antioxidant capability. Therefore, the presence of Sn(IV) contributes to the ester mainly in lipid media than in polar media.

In reactions with the ·OOH radical, which is a more selective radical, the presence of Sn(IV) contributes to significantly improving their antioxidant capability. It could be due to the presence of the Sn(IV) in the deprotonated form, which could contribute to an increase in the angle formed between the plane of the aromatic ring and the lone pair of the oxygen [55], which has been shown to increase the electron donor capability in the antioxidant activity of an antioxidant.

Although this study focuses on evaluating the antioxidant activity, the scope of this study is to contribute to the understanding of the role that the metal plays by being part of an antioxidant compound and enhancing its efficiency, the foregoing to contribute to the development of drugs focused on the treatment of various diseases or conditions in humans, plants or animals in which oxidative stress is an important causative factor, or as antimicrobial, antiviral or antimycotic agents in sanitizing products.

Author Contributions: Conceptualization, R.A.D.-A.; Investigation, R.A.D.-A.; Software Z.G.-S.; Resources Z.G.-S.; Funding Acquisition Z.G.-S. All authors have read and agreed to the published version of the manuscript.

Funding: Conahcyt fellowship 263127, FRABA 804/12 project.

Data Availability Statement: Can be made available upon request from the corresponding author.

Acknowledgments: Z.G.S. acknowledges financial support from FRABA 804/12 and CONAHCyT (CB2008:105721). R.A.D.A. gratefully acknowledges CONAHCyT fellowship 263127.

Conflicts of Interest: The authors declare no conflict of interest.

References

1. Hocman, G. Chemoprevention of cancer: Phenolic antioxidants (BHT, BHA). *Int. J. Biochem.* **1988**, *20*, 639–651. [[CrossRef](#)] [[PubMed](#)]
2. Rotstein, J.B.; Slaga, T.J. Effect of exogenous glutathione on tumor progression in the murine skin multistage carcinogenesis model. *Carcinogenesis* **1998**, *9*, 1547–1551. [[CrossRef](#)] [[PubMed](#)]
3. Perez-Gonzalez, A.; Galano, A. OH Radical Scavenging Activity of Edaravone: Mechanism and Kinetics. *J. Phys. Chem. B* **2011**, *115*, 1306–1314. [[CrossRef](#)] [[PubMed](#)]

4. Corona-Bustamante, A.; Viveros-Paredes, J.M.; Flores-Parra, A.; Peraza-Campos, A.L.; Martínez-Martínez, F.J.; Sumaya-Martínez, M.T.; Ramos-Organillo, A. Antioxidant Activity of Butyl- and Phenylstannoxyanes Derived from 2-, 3- and 4-Pyridinecarboxylic Acids. *Molecules* **2010**, *15*, 5445–5459. [[CrossRef](#)] [[PubMed](#)]
5. Delgado-Alfaro, R.A.; Ramos-Organillo, A.A.; Flores-Moreno, R.; Gómez-Sandoval, Z. Antiradical capacity of a series of organotin(IV) compounds: A chemical reactivity study in the Density Functional Theory framework. *ICA* **2014**, *413*, 143–148. [[CrossRef](#)]
6. Evans, M.G.; Polanyi, M. Some applications of the transition state method to the calculation of reaction velocities, especially in solution. *Trans. Faraday Soc.* **1935**, *31*, 875. [[CrossRef](#)]
7. Evans, M.G.; Polanyi, M. Further considerations on the thermodynamics of chemical equilibria and reaction rates. *Trans. Faraday Soc.* **1936**, *31*, 875. [[CrossRef](#)]
8. Eyring, H. The Activated Complex in Chemical Reactions. *J. Chem. Phys.* **1935**, *3*, 107. [[CrossRef](#)]
9. Eyring, H.; Polanyi, M. Simple Gas Reaction. *Phys. Chem. Abt. B* **1931**, *12*, 279. [[CrossRef](#)]
10. Marcus, R.A. Chemical and Electrochemical Electron-Transfer Theory. *Annu. Rev. Phys. Chem.* **1964**, *15*, 155. [[CrossRef](#)]
11. Hohenberg, P.; Kohn, W. Inhomogeneous Electron Gas. *Phys. Rev. B* **1964**, *136*, 864. [[CrossRef](#)]
12. Kohn, W.; Sham, L.J. Self-Consistent Equations Including Exchange and Correlation Effects. *Phys. Rev. A* **1965**, *140*, A1133–A1138. [[CrossRef](#)]
13. Frisch, M.J.; Trucks, G.W.; Schlegel, H.B.; Scuseria, G.E.; Robb, M.A.; Cheeseman, J.R.; Montgomery, J.A., Jr.; Vreven, T.; Kudin, K.N.; Burant, J.C.; et al. *Gaussian 09*; Version 09; Gaussian, Inc.: Wallingford, CT, USA, 2004.
14. Zhao, Y.; Schultz, N.E.; Truhlar, D.G. Design of Density Functionals by Combining the Method of Constraint Satisfaction with Parametrization for Thermochemistry, Thermochemical Kinetics, and Noncovalent Interactions. *J. Chem. Theory Comput.* **2006**, *2*, 364–382. [[CrossRef](#)] [[PubMed](#)]
15. McLean, A.D.; Chandler, G.S. Contracted Gaussian-basis sets for molecular calculations. 1. 2nd row atoms, Z=11–18. *J. Chem. Phys.* **1980**, *72*, 5639–5648. [[CrossRef](#)]
16. Hay, P.J.; Wadt, W.R. Ab initio effective core potentials for molecular calculations—Potentials for K to Au including the outermost core orbitals. *J. Chem. Phys.* **1985**, *82*, 299–310. [[CrossRef](#)]
17. Hay, P.J.; Wadt, W.R. Ab initio effective core potentials for molecular calculations—Potentials for main group elements Na to Bi. *J. Chem. Phys.* **1985**, *82*, 284–298. [[CrossRef](#)]
18. Hay, P.J.; Wadt, W.R. Ab initio effective core potentials for molecular calculations—Potentials for the transition-metal atoms Sc to Hg. *J. Chem. Phys.* **1985**, *82*, 270–283. [[CrossRef](#)]
19. Zavala-Oseguera, C.; Alvarez-Idaboy, J.R.; Merino, G.; Galano, A. OH Radical Gas Phase Reactions with Aliphatic Ethers: A Variational Transition State Theory Study. *J. Phys. Chem. A* **2009**, *113*, 13913–13920. [[CrossRef](#)]
20. Velez, E.; Quijano, J.; Notario, R.; Pabon, E.; Murillo, J.; Leal, J.; Zapata, E.; Alarcon, G.J. A computational study of stereospecificity in the thermal elimination reaction of methyl benzoate in the gas phase. *Phys. Org. Chem.* **2009**, *22*, 971. [[CrossRef](#)]
21. Galano, A.; Alvarez-Idaboy, J.R. Guanosine + OH radical reaction in aqueous solution: A reinterpretation of the UV-vis data based on thermodynamic and kinetic calculations. *Org. Lett.* **2009**, *11*, 5114. [[CrossRef](#)]
22. Black, G.; Simmie, J.M.J. Barrier heights for H-atom abstraction by HO₂ from n-butanol—A simple yet exacting test for model chemistries? *Comput. Chem.* **2010**, *31*, 1236. [[CrossRef](#)] [[PubMed](#)]
23. Galano, A. Mechanism and kinetics of the hydroxyl and hydroperoxyl radical scavenging activity of N-acetylcysteine amide. *Theor. Chem. Acc.* **2011**, *130*, 51–60. [[CrossRef](#)]
24. Marenich, A.V.; Cramer, C.J.; Truhlar, D.G. Universal Solvation Model Based on Solute Electron Density and on a Continuum Model of the Solvent Defined by the Bulk Dielectric Constant and Atomic Surface Tensions. *J. Phys. Chem. B* **2009**, *113*, 6378–6396. [[CrossRef](#)] [[PubMed](#)]
25. Okuno, Y. Theoretical investigation of the mechanism of the Baeyer–Villiger reaction in nonpolar solvents. *Chem.—Eur. J.* **1997**, *3*, 212–217. [[CrossRef](#)] [[PubMed](#)]
26. Benson, S.W. *The Foundations of Chemical Kinetics*; McGraw-Hill: New York, NY, USA, 1960; pp. 504–508.
27. Ardura, D.; Lopez, R.; Sordo, T.L. Relative Gibbs Energies in Solution through Continuum Models: Effect of the Loss of Translational Degrees of Freedom in Bimolecular Reactions on Gibbs Energy Barriers. *J. Phys. Chem. B* **2005**, *109*, 23618–23623. [[CrossRef](#)] [[PubMed](#)]
28. Alvarez-Idaboy, J.R.; Reyes, L.; Cruz, J. A New Specific Mechanism for the Acid Catalysis of the Addition Step in the Baeyer–Villiger Rearrangement. *Org. Lett.* **2006**, *8*, 1763–1765. [[CrossRef](#)] [[PubMed](#)]
29. Alvarez-Idaboy, J.R.; Reyes, L.; Mora-Diez, N. The mechanism of the Baeyer–Villiger rearrangement: Quantum chemistry and TST study supported by experimental kinetic data. *Org. Biomol. Chem.* **2007**, *5*, 3682–3689. [[CrossRef](#)]
30. Galano, A. Influence of Silicon Defects on the Adsorption of Thiophene-like Compounds on Polycyclic Aromatic Hydrocarbons: A Theoretical Study Using Thiophene + Coronene as the Simplest Model. *J. Phys. Chem. A* **2007**, *111*, 1677–1682. [[CrossRef](#)]
31. Galano, A. Carbon Nanotubes as Free-Radical Antioxidants. *J. Phys. Chem. C* **2008**, *112*, 8922–8927. [[CrossRef](#)]
32. Galano, A.; Cruz-Torres, A. OH radical reactions with phenylalanine in free and peptide forms. *Org. Biomol. Chem.* **2008**, *6*, 732–738. [[CrossRef](#)]
33. Galano, A.; Francisco-Marquez, M. Reactivity of silicon and germanium doped CNTs toward aromatic sulfur compounds: A theoretical approach. *Chem. Phys.* **2008**, *345*, 87–94. [[CrossRef](#)]

34. Mora-Diez, N.; Keller, S.; Alvarez-Idaboy, J.R. The Baeyer–Villiger reaction: Solvent effects on reaction mechanisms. *Org. Biomol. Chem.* **2009**, *7*, 3682–3690. [[CrossRef](#)] [[PubMed](#)]
35. Truhlar, D.G.; Hase, W.L.; Hynes, J.T. Current status of transition-state theory. *J. Phys. Chem.* **1983**, *87*, 2664–2682. [[CrossRef](#)]
36. Truhlar, D.G.; Kuppermann, A. Exact Tunneling Calculations. *J. Am. Chem. Soc.* **1971**, *93*, 1840–1851. [[CrossRef](#)]
37. Chiodo, S.G.; Leopoldini, M.; Russo, N.; Toscano, M. The inactivation of lipid peroxide radical by quercetin. A theoretical insight. *Phys. Chem. Chem. Phys.* **2010**, *12*, 7662–7670. [[CrossRef](#)]
38. Marcus, R.A. Electron transfer reactions in chemistry. Theory and experiment. *Rev. Mod. Phys.* **1993**, *65*, 599. [[CrossRef](#)]
39. Marcus, R.A. Transfer reactions in chemistry. Theory and experiment. *Pure Appl. Chem.* **1997**, *69*, 13–29. [[CrossRef](#)]
40. Collins, F.C.; Kimball, G.E. Diffusion-controlled reaction rates. *J. Colloid Sci.* **1949**, *4*, 425–437. [[CrossRef](#)]
41. Truhlar, D.G. Nearly Encoun11, tri-Controlled Reactions: The Equivalence of the Steady-State and Diffusional Viewpoints. *J. Chem. Ed.* **1985**, *62*, 104–106. [[CrossRef](#)]
42. Einstein, A. Quantum Effect on Elementary Process of Diffusion and Collective Motion of Brown Particles. *Ann. Phys.* **1905**, *17*, 549–560. [[CrossRef](#)]
43. Stokes, G.G. *Mathematical and Physical Papers*; Cambridge University Press: Cambridge, UK, 1903; Volume 3, esp. Sect. IV; p. 55.
44. Leon-Carmona, J.R.; Alvarez-Idaboy, J.R.; Galano, A. On the peroxy scavenging activity of hydroxycinnamic acid derivatives: Mechanisms, kinetics, and importance of the acid–base equilibrium. *Phys. Chem. Chem. Phys.* **2012**, *14*, 12534–12543. [[CrossRef](#)]
45. Ho, J.; Coote, M.L. A universal approach for continuum solvent pKa calculations: Are we there yet? *Theor. Chem. Acc.* **2010**, *125*, 3–21. [[CrossRef](#)]
46. Song, Y.; Zhang, Y.; Shen, T.; Bajaj, C.L.; McCammon, J.A.; Baker, N.A. Finite Element Solution of the Steady-State Smoluchowski Equation for Rate Constant Calculations. *Biophys. J.* **2004**, *86*, 2017–2029. [[CrossRef](#)] [[PubMed](#)]
47. Lee, T.J.; Taylor, P.R. A Diagnostic for Determining the Quality of Single-Reference Electron Correlation Methods. *Int. J. Quant. Chem. Quantum Chem. Symp.* **1989**, *23*, 199–207. [[CrossRef](#)]
48. Pople, J.A.; Head-Gordon, M. Quadratic configuration interaction. A general technique for determining electron correlation energies. *J. Chem. Phys.* **1987**, *87*, 5968–5976. [[CrossRef](#)]
49. Galano, A.; Alvarez-Idaboy, J.R.; Francisco-Márquez, M. Physicochemical Insights on the Free Radical Scavenging Activity of Sesamol: Importance of the Acid/Base Equilibrium. *J. Phys. Chem. B* **2011**, *115*, 13101–13109. [[CrossRef](#)] [[PubMed](#)]
50. Galano, A.; Francisco-Márquez, M. Peroxyl-Radical-Scavenging Activity of Garlic: 2-Propenesulfenic Acid versus Allicin. *J. Phys. Chem. B* **2009**, *113*, 16077–16081. [[CrossRef](#)] [[PubMed](#)]
51. Panhwar, Q.K.; Memon, S.; Bhanger, M.I. Synthesis, characterization, spectroscopic and antioxidation studies of Cu(II)–morin complex. *J. Mol. Struct. (Theochem)* **2010**, *967*, 47–53. [[CrossRef](#)]
52. El-Gammal, O.A.; Bekheit, M.M.; Tahoon, M. Synthesis, characterization and biological activity of 2-acetylpyridine-a-naphthoxyacetylhydrazone its metal complexes. *Spectrochim. Acta Part A Mol. Biomol. Spectrosc.* **2015**, *135*, 597–607. [[CrossRef](#)]
53. Tehrani, Z.A.; Fattahi, A.; Pourjavadi, A. Interaction of Mg²⁺, Ca²⁺, Zn²⁺ and Cu⁺ with cytosine nucleosides: Influence of metal on sugar puckering and stability of N-Glycosidic bond, a DFT study. *J. Mol. Struct. (Theochem)* **2009**, *913*, 117–125. [[CrossRef](#)]
54. Setiadi, D.H.; Chass, G.A.; Torday, L.L.; Varro, A.; Papp, J.G. Vitamin E models. Conformational analysis and stereochemistry of tetralin, chroman, thiochroman and selenochroman. *J. Mol. Struct. (Theochem)* **2002**, *594*, 161–172. [[CrossRef](#)]
55. Denisova, T.G.; Denisov, E.T. Geometric Parameters of the Transition State in Radical Reactions of Antioxidants. *Kin. Catal.* **2004**, *45*, 826–846. [[CrossRef](#)]

Disclaimer/Publisher’s Note: The statements, opinions and data contained in all publications are solely those of the individual author(s) and contributor(s) and not of MDPI and/or the editor(s). MDPI and/or the editor(s) disclaim responsibility for any injury to people or property resulting from any ideas, methods, instructions or products referred to in the content.